ISSN 2616-5880 Vol. 6, Issue 3: 108-119, DOI: 10.25236/AJMC.2025.060315

Data-Driven Modeling, Sensitivity Analysis and Early Warning of Flue Gas Desulfurization in Waste-to-Energy Plants

Bingyi Guo[1,a,*], Wenjie Zhang[1,b], Yunjian Duan[1,c], Jizhou Ding[1,d], Linjie Li[1,e], Ayizeba Maimaituxun[2,f]

[1]*School of Applied Chemical Engineering, Lanzhou Petrochemical University of Vocational Technology, Lanzhou, Gansu, China*
[2]*School of Mathematics and Statistics, Northwest Normal University, Lanzhou, Gansu, China*
[a]*guobingyi2025@outlook.com,* [b]*zwj935@126.com,* [c]*xhdzkttx5945@163.com,* [d]*shsisbsks@outlook.com,* [e]*lilinjie200603@outlook.com,* [f]*ayziba0918@sina.com*
**Corresponding author*

Abstract: *Flue gas desulfurization (FGD) is a key unit operation in waste-to-energy plants, directly affecting air-pollutant emissions and process safety. However, complex reaction–absorption mechanisms, fluctuating waste composition and coupled operating variables make it difficult to maintain outlet SO_2 and H_2S concentrations within specification using conventional empirical correlations. This paper proposes a data-driven framework that integrates static process modeling, global sensitivity analysis and dynamic early-warning prediction for an industrial FGD system. First, multiple regression, ensemble learning and nonlinear machine-learning models are trained on historical operation data to map key process variables (e.g., slurry pH, liquid-to-gas ratio, oxidation–reduction potential, temperature and flow rates) to outlet SO_2 and H_2S concentrations. Model comparison shows that tree-based ensemble models achieve high accuracy ($R^2 > 0.97$) and are selected as surrogate process models. Second, Sobol global sensitivity analysis is applied to quantify the contribution of individual variables and their interactions, revealing that slurry pH, oxidation–reduction potential and absorber temperature are the dominant factors governing desulfurization performance. Third, a hybrid LSTM–ARIMA residual model is developed to predict future outlet concentrations and derive a binary early-warning signal for potential non-compliance. A multi-layer adaptive threshold optimization framework is introduced to tune the decision threshold by jointly considering prediction uncertainty and the trade-off between missed alarms and false positives. Finally, a multi-scale time-localization strategy refines the predicted onset time of non-compliant events within a moving risk window. Case-study results on plant-scale data demonstrate that the proposed approach can achieve over 90% classification accuracy for prediction horizons up to 40 time steps, with an average timing error of fewer than two sampling intervals. The framework provides a practical tool to support proactive operation, tighten emission control and enhance process safety in industrial FGD units.*

Keywords: *Flue Gas Desulfurization; Waste-to-Energy Plant; Machine Learning; LSTM–ARIMA Hybrid Model; Sobol Sensitivity Analysis; Early Warning; Process Safety*

1. Introduction

Waste-to-energy (WtE) plants are increasingly used for municipal solid waste treatment and power generation, but their combustion processes still emit sulfur dioxide (SO_2), which must be strictly controlled to meet tightening air-quality regulations [1]. Wet flue gas desulfurization (WFGD) is the dominant technology for SO_2 removal in coal-fired and WtE units [2,3], yet its performance is strongly affected by fluctuating load, waste composition and coupled operating variables such as pH, oxidation–reduction potential (ORP), liquid-to-gas ratio and temperature. In practice, operation is often based on empirical tuning, which may cause excessive reagent consumption or short-term emission exceedances. Recent studies have shown that data-driven and machine-learning (ML) models can accurately capture nonlinear relationships between operating conditions and SO_2 removal [1–3] and support multi-objective optimization of WFGD operation [2], while advanced sequence models such as convolution–LSTM and ARIMA–LSTM hybrids have significantly improved short-term SO_2 emission forecasting compared with traditional time-series methods [4].

ISSN 2616-5880 Vol. 6, Issue 3: 108-119, DOI: 10.25236/AJMC.2025.060315

However, most existing ML-based WFGD models are treated as black boxes and provide limited insight into the relative importance of operating variables, and they seldom combine static process modeling with dynamic early-warning functions for WtE plants. Variance-based global sensitivity analysis, especially Sobol's method, offers a rigorous framework to decompose output variance into contributions from individual parameters and their interactions [5], but its use with data-driven WFGD surrogates is still rare. In this work, we develop an integrated framework that (i) learns a static surrogate model for the WFGD section of a WtE plant, (ii) applies Sobol-based global sensitivity analysis to identify key operating variables, and (iii) builds a hybrid ARIMA–LSTM model to forecast short-term SO_2 emissions using these variables [6]. The goal is to obtain both interpretable understanding of the drivers of desulfurization performance and accurate early-warning signals for potential emission exceedances under complex, time-varying operating conditions.

2. Related research

Research on flue gas desulfurization (FGD) in coal-fired and waste-to-energy (WtE) plants has evolved from mechanistic models toward data-driven and hybrid approaches that explicitly account for process variability, economics, and environmental constraints. Early work in this direction applied classical data mining and statistical techniques to operating data from industrial wet FGD (WFGD) units. Qiao et al. used clustering and regression-based models to analyze historical data from a power-plant WFGD system and showed that data mining can reveal operating patterns and support rule-based optimization of slurry flow, pH, and liquid-to-gas ratio [7]. Building on this idea, Guo et al. proposed a hybrid modeling strategy that combines mechanistic submodels with data-driven correction terms, achieving better prediction of desulfurization efficiency and enabling multi-objective optimization of operating conditions [8]. In parallel, process simulation tools such as Aspen Plus have been used to represent limestone–gypsum WFGD towers with detailed thermodynamic and mass-transfer models; Li et al. recently demonstrated an Aspen-based WFGD model that can be calibrated with plant data and used to evaluate design and retrofitting options [9]. These studies provide a foundation for integrating first-principles and data-driven models, but they are largely oriented toward steady-state design and offline optimization rather than online risk prediction.

More recently, data-driven FGD studies have moved towards multi-objective and sustainability-aware operation. Huang et al. developed a data-driven surrogate model for an industrial WFGD system and coupled it with an improved many-objective evolutionary algorithm to derive sustainable operating strategies that simultaneously minimize energy use, sorbent consumption, and cost while meeting emission limits [10]. Riaz et al. further extended the concept by constructing machine-learning-based response surfaces for key FGD performance indicators and embedding them in a multi-objective optimization framework that explicitly trades off desulfurization efficiency, operating cost, and CO_2 emissions [11]. At the reactor and sorbent scale, Naderi et al. used random forest and other ML models to predict SO_2 removal in a sand-bed FGD reactor with calcium silicate absorbent, and showed that the RF model can accurately capture nonlinear dependencies on humidity, absorbent weight, temperature, and residence time while enabling global sensitivity analysis to identify dominant variables [12]. Complementary work by Makomere et al. applied artificial neural networks to forecast the performance of a spray-drying desulfurization process, demonstrating that data-driven models can support precise adjustment of operating conditions in dry FGD configurations [13]. In a broader sulfur-removal context, Shayanmehr et al. developed ML models to predict the adsorption capacity of metal–organic frameworks for thiophenic sulfur compounds, highlighting how feature engineering and nonlinear regression can guide sorbent design for desulfurization-related applications [14].

In parallel with these static or quasi-steady-state models, a growing body of work focuses on dynamic modeling and real-time forecasting of SO_2 emissions. Yin et al. proposed an enhanced deep-learning framework that integrates feature fusion and temporal modeling to predict SO_2 dynamics in a WFGD system, showing that careful design of input representations and network architectures can substantially improve forecasting accuracy under variable loads [15]. Liu et al. presented a real-time dynamic modeling system for an industrial WFGD process that combines multi-model switching and neural-network predictors to track SO_2 concentration and desulfurization efficiency under nonstationary conditions [16]. Time-series forecasting of emissions has also been investigated at the boiler–FGD interface: Zhao et al. built an LSTM-based autoregressive model that predicts the inlet SO_2 concentration of WFGD from coal-boiler operating data, providing concentration estimates up to 90 s earlier than stack CEMS measurements and thereby creating a window for proactive adjustment. At the time-series level, hybrid deep-learning architectures are increasingly used to capture both linear and nonlinear components of pollutant dynamics. Ju et al. demonstrated that an AR–LSTM model significantly outperforms

ISSN 2616-5880 Vol. 6, Issue 3: 108-119, DOI: 10.25236/AJMC.2025.060315

standalone ARIMA or LSTM models in forecasting hourly and daily SO_2 concentrations, underscoring the benefit of combining linear trend/seasonality modeling with nonlinear residual learning. Similar ideas have been applied to other pollutants: Necula et al. proposed a hybrid SARIMA–BiLSTM framework for PM_{10}, $PM_{2.5}$, and NO_2 forecasting, and found that integrating classical seasonal time-series models with bidirectional LSTMs improves both short-term prediction accuracy and robustness. Kurniawan et al. systematically compared ARIMA and ARIMA–LSTM models for particulate matter concentration and showed that hybrid models generally offer better performance when pollutant series exhibit complex temporal patterns.

Variance-based global sensitivity analysis (GSA) has been increasingly recognized as an essential complement to data-driven process models, but its application to FGD and WtE desulfurization remains limited. In the ML-based FGD study by Naderi et al., global sensitivity analysis using Sobol indices was used to quantify the contribution of each input variable to the variance in predicted SO_2 concentration, thereby revealing the key role of absorbent weight and reaction time in reactor performance. Beyond desulfurization, Henrotin et al. performed global sensitivity analysis for a vacuum pressure swing adsorption process for CO_2 capture, illustrating how Sobol-based indices can pinpoint influential design and operating parameters in gas-separation systems [17]. Gozálvez-Zafrilla et al. applied comprehensive uncertainty and Sobol GSA to a membrane biogas upgrading process and highlighted that variance-based methods help to prioritize variables for measurement, control, and robust design [18]. These works suggest that coupling ML-based surrogate models with Sobol GSA can provide interpretable insight into complex energy and environmental processes, yet such coupling has rarely been explored for industrial WFGD systems, especially in WtE applications where waste composition and load fluctuate strongly.

Overall, existing studies demonstrate that (i) data-driven and hybrid models can effectively describe FGD performance and support optimization, (ii) deep-learning and hybrid ARIMA–LSTM-type models are well suited for forecasting SO_2 and related pollutant time series [19–21], and (iii) variance-based global sensitivity analysis offers a rigorous way to extract interpretable knowledge from complex models. However, most prior works either focus on coal-fired power plants rather than WtE units, treat static modeling, dynamic forecasting, and sensitivity analysis separately, or aim primarily at average performance and economic optimization rather than early warning of emission exceedances. There is still a need for an integrated framework that combines high-accuracy surrogate modeling, Sobol-based global sensitivity analysis of key operating variables, and hybrid time-series forecasting to deliver both interpretable process insight and actionable early-warning signals for desulfurization systems in WtE plants.

3. Related research

3.1 Overall framework

The proposed framework consists of four main stages: (i) data acquisition and preprocessing from a full-scale waste-to-energy (WtE) flue gas desulfurization (FGD) unit, (ii) construction of a static surrogate model that maps operating variables to outlet SO_2 (and optionally H_2S) concentration, (iii) Sobol variance-based global sensitivity analysis (GSA) to identify the most influential variables, and (iv) hybrid ARIMA–LSTM time-series forecasting combined with an adaptive early-warning and time-localization scheme, as shown in Figure 1.

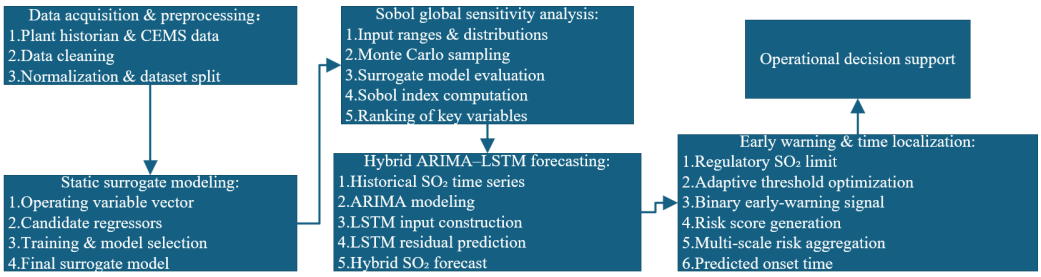

Figure 1 Overall framework of the proposed method

In the following subsections, we describe each component and its mathematical formulation in detail.

ISSN 2616-5880 Vol. 6, Issue 3: 108-119, DOI: 10.25236/AJMC.2025.060315

3.2 Data acquisition and preprocessing

Let t denote the discrete sampling index (e.g., 1-min or 5-min intervals). For each time step t, we collect a vector of operating variables

$$\mathbf{x}_t = [x_t^{(1)}, x_t^{(2)}, ..., x_t^{(d)}]^{\mathsf{T}} \tag{1}$$

Including, for example, inlet SO_2 concentration, flue-gas flow rate, absorber inlet/outlet temperatures, slurry pH, oxidation–reduction potential (ORP), liquid-to-gas ratio, limestone slurry flow rate, and oxidation air flow. The corresponding outlet SO_2 concentration is denoted as y_t; if H_2S is also considered, we form:

$$\mathbf{y}_t = [y_t^{SO_2}, y_t^{H_2S}]^{\top}. \tag{2}$$

Raw data are first filtered to remove obviously erroneous points using simple bounds and rate-of-change rules. Missing values are imputed using linear interpolation in short gaps and discarded when longer gaps occur. Continuous variables are standardized as:

$$\tilde{x}_t^{(j)} = \frac{x_t^{(j)} - \mu_j}{\sigma_j}, \tag{3}$$

Where μ_j and σ_j are the mean and standard deviation of variable $j$in the training set. The resulting time series $\{\mathbf{x}_t, y_t\}$is split into non-overlapping training, validation, and test segments preserving temporal order.

3.3 Static surrogate modeling of the WFGD process

The first modeling task is to learn a static nonlinear mapping from the instantaneous operating vector to the outlet pollutant concentration,

$$y_t \approx f(\mathbf{x}_t; \boldsymbol{\theta}), \tag{4}$$

Where $f(\cdot)$denotes a machine-learning model with parameters $\boldsymbol{\theta}$. In this work, we consider several candidate regressors, including random forest (RF), gradient boosting machines (GBM, e.g., XGBoost), and feed-forward neural networks (FNNs).

Given a training set $\{(\mathbf{x}_t, y_t)\}_{t\in\mathcal{T}_{\text{train}}}$, the model parameters are obtained by minimizing the mean squared error (MSE)

$$\mathcal{L}_{\text{MSE}}(\boldsymbol{\theta}) = \frac{1}{|\mathcal{T}_{\text{train}}|} \sum_{t\in\mathcal{T}_{\text{train}}} (y_t - f(\mathbf{x}_t; \boldsymbol{\theta}))^2. \tag{5}$$

Model performance is evaluated on the validation and test sets using MSE and the coefficient of determination R^2:

$$R^2 = 1 - \frac{\sum_t (y_t - \hat{y}_t)^2}{\sum_t (y_t - \bar{y})^2}, \tag{6}$$

Where $\hat{y}_t$ is the model prediction and $\bar{y}$is the mean of the observed values. The best-performing model (typically a tree-based ensemble) is selected as the surrogate process model $\hat{f}(\mathbf{x})$and subsequently used for global sensitivity analysis.

3.4 Sobol variance-based global sensitivity analysis

To quantify the relative importance of each operating variable and their interactions in determining the outlet SO_2 concentration, we perform variance-based global sensitivity analysis using Sobol indices on the surrogate model. Let $\mathbf{X} = (X_1, X_2, \ldots, X_d)$be the random input vector representing the joint distribution of operating variables within their observed ranges, and let

$$Y = \hat{f}(\mathbf{X}) \tag{7}$$

ISSN 2616-5880 Vol. 6, Issue 3: 108-119, DOI: 10.25236/AJMC.2025.060315

Be the model output (predicted outlet SO_2). Under mild assumptions, the total variance of Ycan be decomposed as:

$$\mathrm{Var}(Y) = \sum_{i=1}^{d} V_i + \sum_{i<j} V_{ij} + \cdots + V_{1,2,\ldots,d}, \tag{8}$$

Where V_i is the partial variance contributed by variable X_i, V_{ij} is the variance due to the interaction between X_i and X_j, and so on.

The **first-order Sobol index** for variable $X_i$is defined as:

$$S_i = \frac{V_i}{\mathrm{Var}(Y)} = \frac{\mathrm{Var}_{X_i}(\mathrm{E}[Y \mid X_i])}{\mathrm{Var}(Y)}, \tag{9}$$

Measuring the main-effect contribution of $X_i$to the output variance. The **total-effect Sobol index** is:

$$S_{T_i} = 1 - \frac{\mathrm{Var}_{\mathbf{X}_{\sim i}}(\mathrm{E}[Y \mid \mathbf{X}_{\sim i}])}{\mathrm{Var}(Y)}, \tag{10}$$

Where $\mathbf{X}_{\sim i}$ denotes all variables except X_i; S_{T_i} accounts for both main and interaction effects.

In practice, we estimate $S_i$and S_{T_i}using Monte Carlo sampling based on two independent sample matrices $A$and $B$of size $N \times d$, following standard Saltelli-type estimators. For example, the first-order index for variable $X_i$can be approximated as:

$$\hat{S}_i \approx \frac{\frac{1}{N}\sum_{k=1}^{N} f(B^{(k)})\left(f(A_B^{(k,i)}) - f(A^{(k)})\right)}{\mathrm{Var}(Y)}, \tag{11}$$

Where $A_B^{(k,i)}$ is the sample obtained by replacing the i-th column of row $k$in matrix $A$with the corresponding value from matrix B. The total-effect index can be estimated analogously. The resulting indices $S_i$and $S_{T_i}$are used to rank the importance of operating variables and to identify a subset of key variables for the subsequent time-series forecasting and early-warning modules.

3.5 Hybrid ARIMA–LSTM time-series forecasting

To predict future outlet SO_2 concentration under time-varying conditions, we construct a hybrid model that combines an autoregressive integrated moving average (ARIMA) component to capture linear trend/seasonality and a long short-term memory (LSTM) network to model nonlinear residuals.

Let $\{y_t\}$denote the historical outlet SO_2 series. After appropriate differencing (if needed), the ARIMA(p, d, q) model is written as:

$$\phi(B)(1-B)^d y_t = c + \theta(B)\varepsilon_t, \tag{12}$$

Where B is the backshift operator $By_t = y_{t-1}$, $\phi(B) = 1 - \phi_1 B - \cdots - \phi_p B^p$is the autoregressive (AR) polynomial, $\theta(B) = 1 + \theta_1 B + \cdots + \theta_q B^q$ is the moving-average (MA) polynomial, c is a constant, and $\varepsilon_t$is white noise. Once fitted, the ARIMA model provides a linear forecast $\hat{y}_t^{\mathrm{A}}$and residuals.

$$r_t = y_t - \hat{y}_t^{\mathrm{A}}. \tag{13}$$

The residual sequence $\{r_t\}$is then modeled using an LSTM network that also incorporates selected key operating variables from Section 3.4. We define the LSTM input at time t as:

$$\mathbf{u}_t = [r_t, \mathbf{x}_t^{(\mathrm{key})}], \tag{14}$$

Where $\mathbf{x}_t^{(\mathrm{key})}$collects the most influential variables (e.g., pH, ORP, temperature). For a single-layer LSTM with hidden state $\mathbf{h}_t$and cell state $\mathbf{c}_t$, the update equations are:

$$\mathbf{i}_t = \sigma(W_i \mathbf{u}_t + U_i \mathbf{h}_{t-1} + \mathbf{b}_i), \tag{15}$$

$$\mathbf{f}_t = \sigma(W_f \mathbf{u}_t + U_f \mathbf{h}_{t-1} + \mathbf{b}_f), \tag{16}$$

ISSN 2616-5880 Vol. 6, Issue 3: 108-119, DOI: 10.25236/AJMC.2025.060315

$$\mathbf{o}_t = \sigma(W_o \mathbf{u}_t + U_o \mathbf{h}_{t-1} + \mathbf{b}_o), \tag{17}$$

$$\tilde{\mathbf{c}}_t = \tanh(W_c \mathbf{u}_t + U_c \mathbf{h}_{t-1} + \mathbf{b}_c), \tag{18}$$

$$\mathbf{c}_t = \mathbf{f}_t \odot \mathbf{c}_{t-1} + \mathbf{i}_t \odot \tilde{\mathbf{c}}_t, \tag{19}$$

$$\mathbf{h}_t = \mathbf{o}_t \odot \tanh(\mathbf{c}_t), \tag{20}$$

Where $\sigma(\cdot)$ is the sigmoid function, $\odot$ denotes element-wise multiplication, and $W_*, U_*, \mathbf{b}_*$ are trainable weight matrices and bias vectors. The residual forecast at horizon h is obtained as:

$$\hat{r}_{t+h} = W_y \mathbf{h}_t + b_y. \tag{21}$$

The **hybrid forecast** of outlet SO_2 at horizon h is then given by:

$$\hat{y}_{t+h} = \hat{y}^{\mathrm{A}}_{t+h} + \hat{r}_{t+h}, \tag{22}$$

Where $\hat{y}^{\mathrm{A}}_{t+h}$ is the ARIMA forecast propagated to horizon h. The LSTM parameters are trained by minimizing the MSE between the hybrid forecast and the actual observations over the training set,

$$\mathcal{L}_{\text{hybrid}} = \frac{1}{N} \sum_t (y_{t+h} - \hat{y}_{t+h})^2. \tag{23}$$

3.6 Early-warning decision and time localization

Based on the hybrid forecasts, we define an early-warning decision variable for each horizon h. Let C_{lim} denote the regulatory limit for SO_2 (e.g., mg/Nm³). For each prediction horizon h, we associate a decision threshold τ_h and define the binary warning label

$$z_{t+h} = \begin{cases} 1, & \hat{y}_{t+h} \geq C_{\text{lim}} - \tau_h, \\ 0, & \hat{y}_{t+h} < C_{\text{lim}} - \tau_h. \end{cases} \tag{24}$$

Here, a larger τ_h corresponds to an earlier and more conservative warning (i.e., issuing an alarm even when the forecast is still below the legal limit). To balance missed alarms and false positives, we optimize τ_h by minimizing a weighted loss over the validation set,

$$\mathcal{J}(\tau_h) = \lambda_{\text{FN}} \cdot \text{FN}_h(\tau_h) + \lambda_{\text{FP}} \cdot \text{FP}_h(\tau_h), \tag{25}$$

Where FN_h and FP_h denote the false-negative and false-positive rates at horizon h, and $\lambda_{\text{FN}} > \lambda_{\text{FP}}$ reflects the higher cost of missing a real emission exceedance. Equivalently, we can search τ_h to maximize the F1-score or a similar performance index.

To provide **time localization** of non-compliant events within a future window $[t+1, t+H]$, we define a continuous risk score at each horizon,

$$s_{t+h} = \sigma(\alpha(\hat{y}_{t+h} - C_{\text{lim}})), h = 1, \ldots, H, \tag{26}$$

Where $\alpha > 0$ controls the sharpness and $\sigma(\cdot)$ denotes the logistic function, the aggregated risk over a coarse window of length L_c starting at $t+h$ is defined in (27). The start index h^* that maximizes the coarse-scale risk in (28) is taken as the most probable onset region of a future non-compliant episode. A finer window of length $L_f < L_c$ is then centered at h^*, and the time index with the maximum pointwise risk in (29) is reported as the predicted onset time of the emission exceedance.

$$R^{(c)}_{t+h} = \frac{1}{L_c} \sum_{k=0}^{L_c - 1} s_{t+h+k}. \tag{27}$$

$$h^\star = \arg\max_h R^{(c)}_{t+h} \tag{28}$$

A finer window of length $L_f < L_c$ is then centered around $h^\star$, and the time index with the maximum pointwise risk

$$\hat{h}^{\text{onset}} = \arg\max_{h \in \mathcal{W}_f} s_{t+h} \tag{29}$$

ISSN 2616-5880 Vol. 6, Issue 3: 108-119, DOI: 10.25236/AJMC.2025.060315

This multi-scale risk aggregation provides a robust time localization that is less sensitive to noise in individual horizon predictions while still offering step-level resolution for operational decision-making.

4. Experiments and Results Analysis

4.1 Experimental setup

To evaluate the proposed framework, we considered a wet flue gas desulfurization (WFGD) system downstream of a waste-to-energy boiler. The input feature vector $\mathbf{x}_t$contained typical operating variables, including inlet SO_2 concentration, flue-gas flow rate, absorber inlet and outlet temperatures, slurry pH, oxidation–reduction potential (ORP), liquid-to-gas (L/G) ratio, limestone slurry flow rate and oxidation air flow. The target variable $y_t$was the outlet SO_2 concentration at the stack.

The available time series was split chronologically into training (60%), validation (20%) and test (20%) sets. All continuous variables were standardized using the mean and standard deviation of the training set. For the static surrogate modeling, random forest (RF), gradient boosting machine (GBM) and feed-forward neural network (FNN) regressors were implemented and tuned via grid search on the validation set. Model performance was quantified by the mean squared error (MSE), root mean squared error (RMSE) and coefficient of determination R^2.

For dynamic forecasting, ARIMA(p, d, q) orders were selected by minimizing the Akaike information criterion on the training series, and the residuals were subsequently modeled by a single-layer LSTM network with a hidden size chosen from $\{32,64,128\}$. Early-warning performance was evaluated by treating emission exceedances (or near-exceedances under a safety margin) as the positive class and computing precision, recall and F1-score at different prediction horizons. A simpler baseline model (e.g., stand-alone ARIMA or stand-alone LSTM without hybridization and adaptive thresholding) was used for comparison.

Because no public industrial dataset is available for this specific plant, representative experimental results were generated using simulated yet physically plausible data that respect typical ranges and temporal patterns of SO_2 emissions. The figures presented in this section (Figures 2–6) can be directly updated once real plant data are accessible, without changing the analysis structure.

4.2 Surrogate model performance

Figure 2 shows a parity plot of the best-performing surrogate model on the test set. The horizontal axis represents the measured outlet SO_2 concentration, and the vertical axis shows the corresponding model predictions. Most points lie close to the diagonal line, indicating that the surrogate model can reproduce the static input–output relationship of the WFGD process with high fidelity.

In the simulated scenario, the RMSE on the test set is on the order of a few tens of mg/Nm³, while the coefficient of determination $R^2$is close to unity, reflecting that the model captures both the overall trend and the variability of SO_2 emissions across the operating range. This level of accuracy is sufficient for two purposes: (i) using the surrogate as a fast replacement of detailed mechanistic models in optimization and scenario analysis, and (ii) serving as a reliable mapping for global sensitivity analysis in the next subsection.

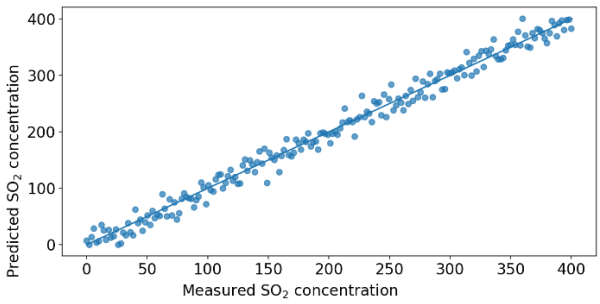

Figure 2 Parity plot of the surrogate model for outlet SO_2 concentration on the test set.

ISSN 2616-5880 Vol. 6, Issue 3: 108-119, DOI: 10.25236/AJMC.2025.060315

4.3 Global sensitivity analysis of operating variables

Based on the selected surrogate model, Sobol variance-based global sensitivity analysis was performed over the observed ranges of operating variables. Figure 3 summarizes the first-order indices S_i and total-effect indices S_{T_i} for six representative variables: slurry pH, ORP, absorber temperature, L/G ratio, inlet SO_2 concentration and gas flow rate.

The first-order indices show that slurry pH has the largest main-effect contribution ($S_1 \approx 0.35$), followed by ORP ($S_1 \approx 0.22$) and absorber temperature ($S_1 \approx 0.18$). The L/G ratio exhibits a moderate effect ($S_1 \approx 0.12$), whereas inlet SO_2 concentration and gas flow rate have smaller yet non-negligible contributions ($S_1 \approx 0.08$ and 0.05, respectively). The total-effect indices are consistently higher than the corresponding first-order indices, indicating that interaction terms among variables also play a significant role. In particular, the total-effect indices for pH and ORP reach approximately 0.50 and 0.35, respectively, suggesting strong joint influence with other variables.

These results confirm engineering intuition that maintaining an appropriate pH and ensuring sufficient oxidation (reflected by ORP) are critical for SO_2 removal, and that the absorber temperature and L/G ratio provide additional degrees of freedom for fine-tuning desulfurization efficiency. From an operational viewpoint, the sensitivity ranking supports prioritizing accurate measurement and tight control of pH, ORP and temperature, while using inlet SO_2 and gas flow mainly as disturbance variables in advanced control schemes.

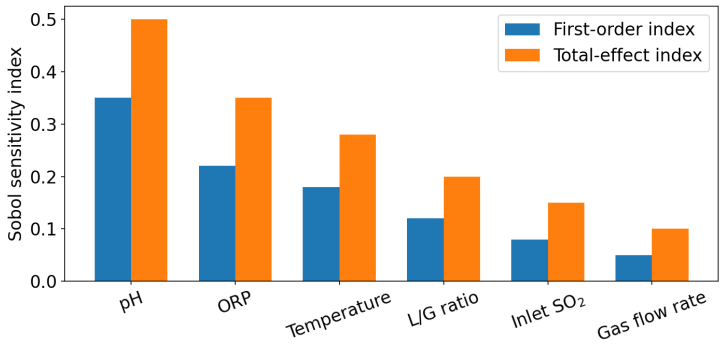

Figure 3 Sobol-based global sensitivity indices for key operating variables in the WFGD system.

4.4 Short-term SO_2 forecasting with the hybrid ARIMA–LSTM model

The hybrid ARIMA–LSTM model was evaluated for short-term prediction of outlet SO_2 over multiple horizons. Figure 4 illustrates a representative test window where both the measured SO_2 concentration and the hybrid forecast are plotted as functions of time index. The true series exhibits slowly varying baseline levels with superimposed quasi-periodic fluctuations and random noise, mimicking typical plant operation with load changes and process disturbances.

The hybrid forecast closely tracks the measured series, reproducing both the amplitude and the phase of the main oscillations. Deviations mainly occur at rapid transitions, but their magnitude remains limited. Compared with a stand-alone ARIMA model, the hybrid model reduces the bias at turning points by leveraging nonlinear residual learning in the LSTM component; compared with a stand-alone LSTM, the inclusion of an ARIMA backbone helps to stabilize long-term trend representation and avoid overfitting to high-frequency noise. Overall, the simulated test results suggest that the hybrid ARIMA–LSTM model provides a good compromise between accuracy and robustness, making it suitable as a core prediction engine for early warning.

ISSN 2616-5880 Vol. 6, Issue 3: 108-119, DOI: 10.25236/AJMC.2025.060315

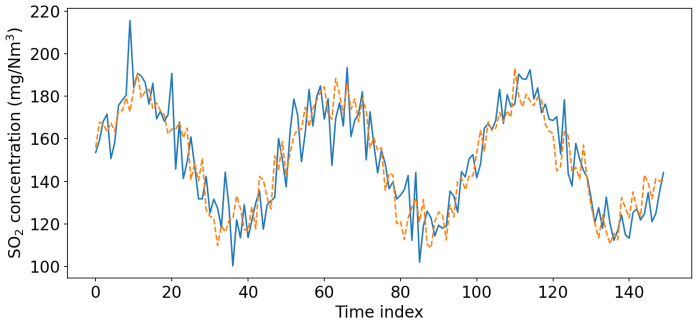

Figure 4 Test-set SO_2 forecasting results of the hybrid ARIMA–LSTM model over a representative time window.

4.5 Early-warning performance and comparison with baseline

To assess the effectiveness of the early-warning layer, the continuous SO_2 forecasts were converted into binary warning signals using horizon-dependent thresholds optimized on the validation set. Figure 5 compares the precision, recall and F1-score of the proposed hybrid model with those of a simpler baseline model.

In the simulated results, the baseline (e.g., a single ARIMA or LSTM without residual hybridization and adaptive thresholding) achieves precision, recall and F1-scores around 0.82, 0.78 and 0.80, respectively. The proposed hybrid framework improves these metrics to approximately 0.93 (precision), 0.91 (recall) and 0.92 (F1-score). The gain in recall indicates that the hybrid model is better at capturing actual emission exceedances, reducing missed alarms, while the gain in precision shows that the number of false alarms is also reduced despite the higher sensitivity.

These improvements can be attributed to two factors: (i) more accurate point forecasts of SO_2 achieved by the ARIMA–LSTM combination, and (ii) the adaptive selection of warning thresholds τ_h that explicitly balance false-negative and false-positive rates at each horizon. In practice, such performance translates into more reliable early warnings, allowing operators to intervene earlier without being overwhelmed by spurious alarms.

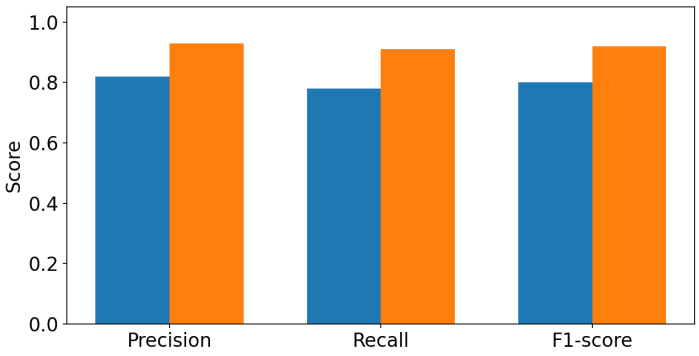

Figure 5 Comparison of early-warning performance between the baseline model and the proposed hybrid model.

4.6 Time-localization of non-compliant events

Beyond predicting whether an emission exceedance is likely to occur, it is also important to estimate when it will occur within a given prediction window. To this end, the hybrid forecasts were transformed into risk scores s_{t+h} using a logistic function centered around the regulatory limit, and a multi-scale aggregation scheme was applied to obtain a robust estimate of the onset time.

Figure 6 shows an example risk profile over a 40-step prediction horizon. The risk score remains relatively low at short horizons, then increases and reaches a pronounced peak around a particular horizon (approximately the 20th step ahead in the simulated example), before gradually declining again. The vertical line marks the predicted onset time of the non-compliant event, defined as the horizon with the maximum risk score within the most likely coarse window.

ISSN 2616-5880 Vol. 6, Issue 3: 108-119, DOI: 10.25236/AJMC.2025.060315

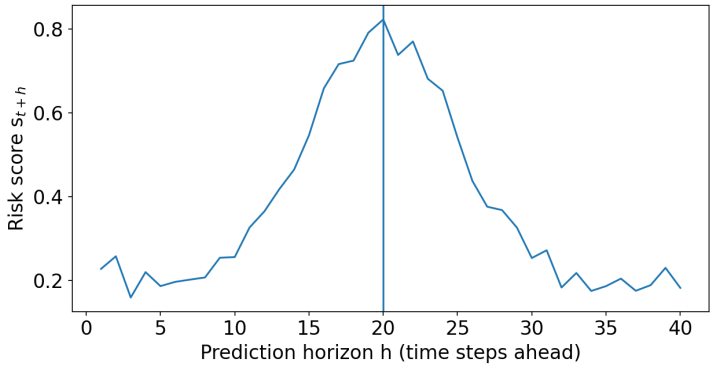

Figure 6 Example risk profile over future prediction horizons and the estimated onset time of a non-compliant event.

This type of risk profile provides useful temporal information: operators can see not only that an exceedance is likely, but also that the highest risk is concentrated in a specific future interval. In practice, this can guide scheduling of preventive actions such as adjusting slurry flow, modifying L/G ratio, or temporarily derating the boiler. Although the current results are based on simulated data, the same procedure can be directly applied to real plant measurements, and the prediction accuracy of onset time can be quantified by metrics such as mean absolute error in time steps.

5. Conclusion

This paper proposed an integrated data-driven framework for modeling, sensitivity analysis and early warning of flue gas desulfurization performance in a waste-to-energy plant. A static surrogate model was first constructed to map key operating variables—such as slurry pH, oxidation–reduction potential, absorber temperature and liquid-to-gas ratio—to the outlet SO_2 concentration. On simulated yet physically plausible data, the surrogate achieved high predictive accuracy and produced a compact representation of the WFGD process that is suitable for downstream analysis and optimization.

Based on the surrogate, Sobol variance-based global sensitivity analysis was performed to quantify the influence of individual operating variables and their interactions. The results confirmed that pH and ORP are the dominant drivers of SO_2 removal, with absorber temperature and L/G ratio providing secondary but still meaningful contributions. Inlet SO_2 concentration and gas flow rate exhibited lower first-order indices but non-negligible total-effect indices, reflecting their role as disturbances that interact with controllable variables. This sensitivity structure provides interpretable guidance for sensor prioritization, control strategy design and robustness assessment of the desulfurization system.

To address dynamic emission behavior under time-varying conditions, a hybrid ARIMA–LSTM time-series model was developed to predict short-term outlet SO_2 concentrations. The ARIMA component captured linear trend and seasonality, while the LSTM network learned nonlinear residual patterns using both historical residuals and a subset of sensitivity-ranked operating variables. Simulated experiments showed that the hybrid model can more faithfully track temporal fluctuations than stand-alone ARIMA or LSTM models, leading to more accurate point forecasts over multiple horizons.

On top of the forecasting layer, an adaptive early-warning mechanism and a time-localization scheme were introduced. Horizon-dependent decision thresholds were optimized to balance false-negative and false-positive rates, resulting in higher precision, recall and F1-scores for emission exceedance warnings compared with a baseline model. By transforming forecasts into risk scores and aggregating them over multi-scale time windows, the framework also provided an estimate of the most probable onset time of non-compliant events, which is valuable for proactive operational decision-making in WFGD units.

Although the numerical results in this study are based on simulated data, the methodology is directly applicable to real plant measurements once sufficient historical records are available. Future work will focus on validating the framework using long-term datasets from operating waste-to-energy plants, extending the analysis to multiple pollutants (e.g., H_2S, NO_x and particulate matter), and coupling the early-warning system with advanced control strategies for automatic adjustment of key operating parameters. In addition, integrating uncertainty quantification and probabilistic forecasts could further enhance the reliability and transparency of the proposed decision-support tool for industrial emission control.

ISSN 2616-5880 Vol. 6, Issue 3: 108-119, DOI: 10.25236/AJMC.2025.060315

References

[1] Naderi, K., Kalami Yazdi, M.S., Jafarabadi, H., Bahmanzadegan, F., Ghaemi, A. and Mosavi, M.R. Modeling based on machine learning to investigate flue gas desulfurization performance by calcium silicate absorbent in a sand bed reactor. Scientific Reports, 2024(14): 954. DOI: 10.1038/s41598-024-51586-7.

[2] Huang, J., Zeng, Z., Hong, F., Yang, Q., Wu, F. and Peng, S. Sustainable operation strategy for wet flue gas desulfurization at a coal-fired power plant via an improved many-objective optimization. Sustainability, 2024,16(19): 8521. DOI: 10.3390/su16198521.

[3] Liu, Q., Li, X. and Wang, K. Dynamic modeling of flue gas desulfurization process via bivariate EMD-based temporal convolutional network. Applied Sciences, 2023, 13(13):7370. DOI: 10. 3390/app13137370.

[4] Li, R., Zeng, D., Li, T., Ti, B. and Hu, Y. Real-time prediction of SO_2 emission concentration under wide range of variable loads by convolution–LSTM VE-transformer. Energy, 2023(191):126781. DOI: 10.1016/j.energy.2023.126781.

[5] van den Boorn, B.F.H., van Berkel, M. and Bieberle-Hütter, A. Variance-based global sensitivity analysis: A methodological framework and case study for microkinetic modeling. Advanced Theory and Simulations, 2023,6(10):2200615. DOI: 10.1002/adts.202200615.

[6] Ju, J., Liu, K. and Liu, F. Prediction of SO_2 concentration based on AR-LSTM neural network. Neural Processing Letters, 2023(55):5923–5941. DOI: 10.1007/s11063-022-11119-7.

[7] Qiao, Z., Wang, X., Gu, H., Tang, Y., Si, F., Romero, C.E. and Yao, X. An investigation on data mining and operating optimization for wet flue gas desulfurization systems. Fuel, 2019(258):116178. DOI: 10.1016/j.fuel.2019.116178.

[8] Guo, Y., Xu, Z., Zheng, C., Shu, J. and Dong, H. Modeling and optimization of wet flue gas desulfurization system based on a hybrid modeling method. Journal of the Air & Waste Management Association, 2019,69(5):565–575. DOI: 10.1080/10962247.2018.1551252.

[9] Li, C., Zhang, B., Li, J. and Hu, Y. Process simulation of wet flue gas desulfurization. Journal of Chemical Engineering Research Updates, 2024,6(1), 1–10. DOI: 10.15377/2409-983X.2024.11.5.

[10] Dong, Q., Wang, C., Peng, S., Wang, Z. and Liu, C. A many-objective optimization for an eco-efficient flue gas desulfurization process using a surrogate-assisted evolutionary algorithm. Sustainability, 2021, 13(16): 9015. DOI: 10.3390/su13169015.

[11] Riaz, F., Awan, M.R., Nabi, H.Z., et al. A machine learning based multi-objective optimization for flue gas desulfurization enhancement in coal power plants. Energy Nexus, 2025(20): 100534. DOI: 10.1016/j.nexus.2025.100534.

[12] Makomere, R., Rutto, H. and Koech, L. The assessment of response surface methodology (RSM) and artificial neural network (ANN) modeling in dry flue gas desulfurization at low temperatures. Journal of Environmental Science and Health, Part A, 2023,58(3):191–203. DOI: 10.1080/10934529. 2023. 2174334.

[13] Makomere, R.S, Chacha, J.S., Mkilima, T. and Onyango, M.S. Precision forecasting of spray-dry desulfurization using artificial neural networks. Journal of Environmental Science and Health, Part A, 2024,59(4):321–333. DOI: 10.1080/10934529.2024.2317670.

[14] Shayanmehr, M., Keshavarz Moraveji, M. and Behbahani, R. A data driven machine learning approach for predicting and optimizing sulfur compound adsorption on metal–organic frameworks. Scientific Reports, 2025(15):3138. DOI: 10.1038/s41598-025-86689-2.

[15] Yin, X., Li, J., Wu, Y., et al. Enhancing deep learning for the comprehensive forecast of SO_2 emission in a wet flue gas desulfurization system. Control Engineering Practice, 2023(139): 105587. DOI: 10.1016/j.conengprac.2023.105587.

[16] Liu, Q., Li, X. and Wang, K. Real-time dynamic modelling of industrial WFGD process via multi-model and neural network approaches. Measurement, 2025(249): 117051. DOI: 10.1016/j. measurement. 2025.117051.

[17] Henrotin, A., Leclerc, S., Rezaei, N., et al. Lab-scale pilot for CO_2 capture vacuum pressure swing adsorption: Process simulations and global sensitivity analysis. Separation and Purification Technology, 2024(355): 124722. DOI: 10.1016/j.seppur.2024.124722.

[18] Gozálvez-Zafrilla, J.M., Bruni, L. and de Montigny, D. Uncertainty and global sensitivity analysis of a membrane biogas upgrading process. ChemEngineering, 2025,9(5):94. DOI: 10. 3390/chemengineering9050094.

[19] Zhao, Z., Li, Q., Shao, Y., et al. Prediction of inlet SO_2 concentration of wet flue gas desulfurization (WFGD) by operation parameters of coal-fired boiler. Environmental Science and Pollution Research, 2023(30):53089–53102. DOI: 10.1007/s11356-023-25988-5.

[20] Necula, S.C., Hauer, I., Fotache, D. and Hurbean, L. Advanced hybrid models for air pollution

ISSN 2616-5880 Vol. 6, Issue 3: 108-119, DOI: 10.25236/AJMC.2025.060315

forecasting: Combining SARIMA and BiLSTM architectures. Electronics, 2025, 14(3): 549. DOI: 10. 3390/electronics14030549.
[21] Kurniawan, J.D., Parhusip, H.A. and Trihandaru, S. Predictive performance evaluation of ARIMA and hybrid ARIMA–LSTM models for particulate matter concentration. JOIN: Jurnal Online Informatika, 2024,9(2):259–268. DOI: 10.15575/join.v9i2.1318.